THEORETICAL AND APPLIED MECHANICS
Volume 45 (2018) Issue 1, 53–65 DOI: https://doi.org/10.2298/TAM171130004S

ESTIMATION OF WIND TURBINE BLADE AERODYNAMIC PERFORMANCES COMPUTED USING DIFFERENT NUMERICAL APPROACHES

Jelena Svorcan, Ognjen Peković, and Toni Ivanov

Abstract. Although much employed, wind energy systems still present an open, contemporary topic of many research studies. Special attention is given to precise aerodynamic modeling performed in the beginning since overall wind turbine performances directly depend on blade aerodynamic performances. Several models different in complexity and computational requirements are still widely used. Most common numerical approaches include: i) momentum balance models, ii) potential flow methods and iii) full computational fluid dynamics solutions.

Short explanations, reviews and comparison of the existing computational concepts are presented in the paper. Simpler models are described and implemented while numerous numerical investigations of isolated horizontal-axis wind turbine rotor consisting of three blades have also been performed in ANSYS FLUENT 16.2. Flow field is modeled by Reynolds Averaged Navier–Stokes (RANS) equations closed by two different turbulence models.

Results including global parameters such as thrust and power coefficients as well as local distributions along the blade obtained by different models are compared to available experimental data. Presented results include fluid flow visualizations in the form of velocity contours, sectional pressure distributions and values of power and thrust force coefficients for a range of operational regimes. Although obtained numerical results vary in accuracy, all presented numerical settings seem to slightly under- or over-estimate the global wind turbine parameters (power and thrust force coefficients). Turbulence can greatly affect the wind turbine aerodynamics and should be modeled with care.

1. Introduction

For its numerous advantages and renewability, wind energy extraction and usage exploration is an open and common topic nowadays. Various, both numerical and experimental studies trying to increase the efficiency of the wind turbines and accurately describe the surrounding flow field have been performed [1–9].

Due to the presence of many flow phenomena, e.g. unsteadiness, tip vortex formation, 3D dynamic stall, blade-vortex interaction etc., flow field is hard to

2010 *Mathematics Subject Classification:* 76-04; 76F60; 76M23.
Key words and phrases: wind turbine, BEMT, vortex methods, turbulence, RANS.

both measure and simulate [10]. Obtaining a usable, sufficiently accurate numerical solution is a difficult task [11]. Several numerical approaches different in complexity and accuracy are generally employed.

Most practical to use is the model based on conservation laws (MT) combined with blade element theory (BET). This combined theory (BEMT) can adequately be used for prediction of aerodynamic performances acting on the blade at steady flow and at medium values of tip-speed ratio $\lambda = \Omega R/V_0$. It is also quite popular for its computational speed and ease of implementation [12]. However, one of its greatest drawbacks is that it relies on available 2D airfoil data. Some examples of its application can be found in [8, 12].

On the other hand, the vortex theory, assuming potential (incompressible, inviscid and irrotational) flow has successfully been applied in estimating aerodynamic properties of aircrafts, finite wings and blades [13, 14]. It can also be combined with tabulated 2D airfoil characteristics to partially account for viscous effects. Compared to BEMT, it is more computationally expensive, but provides more accurate results, is valid for a wider range of tip-speed ratios and allows the consideration of unsteady wind velocities (of changeable direction). When simulating rotating machinery, there are two possible research approaches: modeling the wake as restricted/rigid or free. The latter model considers the wake geometry deformation, generally predicts aerodynamic loads more accurately and can be used as a predictive tool and is therefore investigated in this paper.

While CFD methods (here this term implies full Navier–Stokes equations) are supposed to offer the most accurate and detailed results, they are at the same time the most computationally demanding of all numerical approaches used for prediction of rotor aerodynamic performances. Due to the curved and complex geometry as well as the need to resolve the rotational motion of the blades, each computation requires extensive computational time. In addition, considering turbulence produced by the turbine greatly increases the complexity of the simulations [12].

Due to the great complexity of the considered problem several assumptions were adopted. Upstream flow is uniform and perpendicular to rotor plane. Blades are considered rigid and aeroelastic effects are neglected. The presence of the hub, tower and nacelle is not included in the study, and only the streamlined part of the blades is modeled. These simplifications present an additional difficulty to comparison to available experimental data.

2. Experiment and model description

2.1. Experiment. An instrumented 3-bladed machine, MEXICO experimental wind turbine, with horizontal axis and a 4.5 m rotor diameter is used as a reference [8]. Experimental data are obtained in relatively recent wind tunnel tests under a European Union project [4], Figure 1a. Twist and chord distributions along the blade are illustrated in Figure 1b. Three different airfoils are used on the real blade: DU91-W2-250 from 20–45.6% span, RISØ-A1-21 from 54.4–65.6% span and NACA 64–418 from 74.4% span to the blade tip, Figure 2a. Smooth transition is made between different airfoil shapes.

a) 

b) 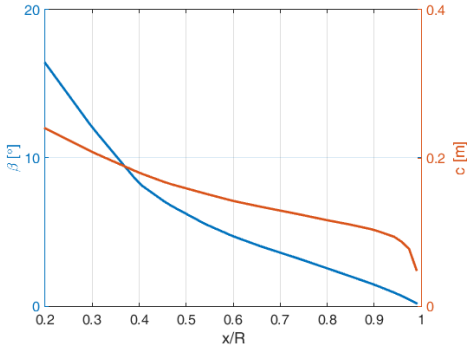

FIGURE 1. a) MEXICO experiment (taken from [4]), b) MEXICO blade twist and chord distributions

Since abundant experimental work has been performed only a portion of experimental data have been used for comparison to computational results. Rotor angular velocity was $\Omega = 324.5$ RPM, resulting in a tip speed of $V_{\text{tip}} = 76\,\text{m/s}$. Different working regimes $\lambda = V_{\text{tip}}/V_0$ are obtained by varying undisturbed wind speed V_0. Its three characteristic values $V_0 = 10,\ 15$ and $24\,\text{m/s}$ represent the turbulent wake state, design operational regime and separated flow conditions respectively [8]. Blade collective pitch angle is $-2.3°$.

a) 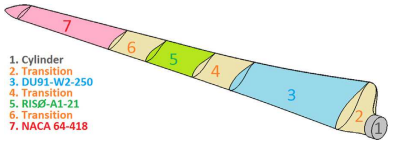

b) 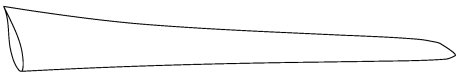

FIGURE 2. a) MEXICO blade airfoil distribution (taken from [8], b) Blade model used in simulations

2.2. Model description. Prior to the description of aerodynamic models, several fundamental variables should be introduced and basic flow conditions explained (Figure 3).

If the flow is considered axis-symmetric wind turbine performances can be estimated from a single representative blade. The rotor is described by the rotor radius R and number of blades N_b. Local chord c varies along the blade. Twist distribution β presents the angle between the local chord and rotor plane (xy-plane in Figure 3).

Many numerical approaches require the division of the blade into segments where each blade element is determined by the local relative coordinate $r = x/R$. The total air velocity relative to the blade segment $\mathbf{V}_{\text{rel}}$ presents the sum of free-stream $\mathbf{V}_0$, tangential (rotational) $\mathbf{\Omega} \times \mathbf{r}$ and induced velocities $\mathbf{v}_i$. The manner

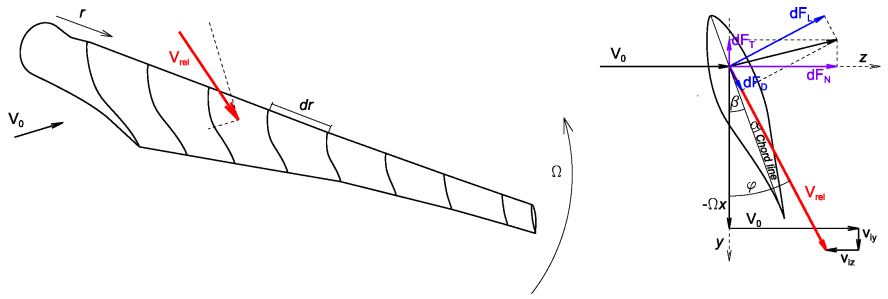

FIGURE 3. Blade model with characteristic velocities and angles

in which these induced velocities are computed is what makes the distinction between the considered numerical approaches. The existence of induced velocities causes the modification of angle-of-attack $\alpha = \phi - \beta$, therefore affecting both lift $F'_L = 0.5\rho V^2_{\text{rel}} c C_L$ and drag $F'_D = 0.5\rho V^2_{\text{rel}} c C_D$ line forces. These forces can be transformed into normal F_N (thrust) and tangential components F_T (affecting power).

3. Computational models

3.1. Blade element momentum theory (BEMT). Relatively simple and quick BEMT model combines Momentum Theory (where rotor is considered as a disc able to absorb energy from wind by reducing its speed along the streamline) and Blade Element Model (where blade is divided into elements that can be considered separately) and is extensively used for preliminary assessments of aerodynamic performances of wind turbines in axial steady flows. Similar to [12], a number of correction functions have been added to the model to account for blade finiteness (overall root and tip losses) and small wind speeds (Advanced brake state model offers a quadratic approximation of a relation between a and $C_{T,MT}$ for $a > 0.4$). Wind shear effect (change of wind velocity due to earth boundary layer) has been neglected at this point.

In MT, change of velocity is presented by induction factors: axial $a = v_{iz}/V_0$ and tangential $a' = v_{iy}/\Omega x$. Relative velocity V_{rel} can then be expressed as:

$$V_{\text{rel}} = \sqrt{[V_0(1-a)]^2 + [\Omega x(1+a')]^2},$$

while the local flow angle ϕ (between the rotor plane and the direction of the relative wind velocity) is:

$$\tan\phi = \frac{(1-a)V_0}{(1+a')\Omega x} = \frac{1-a}{(1+a')r\lambda}.$$

Local inflow angle can now be computed $\alpha = \phi - \beta$, and by using available 2D aerodynamic characteristics, local lift and drag coefficients (BET), as well as normal and tangential force coefficients, can be computed as:

$$C_N = C_L\cos\phi + C_D\sin\phi,$$
$$C_T = C_L\sin\phi - C_D\cos\phi.$$

Total thrust and torque acting on N_b blade elements are then, respectively:

$$\mathrm{d}T_{BET} = \mathrm{d}T_{MT} \iff N_b \tfrac{1}{2}\rho V_{\mathrm{rel}}^2 (C_L \cos\phi + C_D \sin\phi) c \mathrm{d}x = 4\pi x \rho V_0^2 a(1-a)\mathrm{d}x,$$
$$\mathrm{d}Q_{BET} = \mathrm{d}Q_{MT} \iff N_b \tfrac{1}{2}\rho V_{\mathrm{rel}}^2 (C_L \sin\phi - C_D \cos\phi) x c \mathrm{d}x = 4\pi x^3 \rho V_0 \Omega a'(1-a)\mathrm{d}x.$$

By equating these two sets of expressions, it is possible to iteratively solve the induction factors. After reaching the converged solutions, total rotor thrust, torque and power can be computed by summation:

$$T = \sum \mathrm{d}T, Q = \sum \mathrm{d}Q, P = \Omega Q.$$

All the necessary explanations can be found in [12].

3.2. Simplified vortex lattice method (VLM). Potential flow methods are based on superimposing a finite number of fundamental solutions of Laplace's equation to obtain a flow field corresponding to initial geometry [14, 15]. Depending on the type of the chosen fundamental solution a number of methods can be obtained. Here, straight vortex filament is chosen and the induced velocity $\mathbf{v}_i$ is computed by Biot-Savart law:

$$\mathbf{v}_i = \frac{\Gamma}{4\pi} \frac{(r_1 + r_2)(\mathbf{r}_1 + \mathbf{r}_2)}{r_1 r_2 (r_1 r_2 + \mathbf{r}_1 \cdot \mathbf{r}_2) + (\delta l_0)^2},$$

where Γ is vortex intensity and $\mathbf{r}_1$ and $\mathbf{r}_2$ are distance vectors from the beginning and the end of the vortex segment respectively. The additional part in the denominator $(\delta l_0)^2$ serves to prevent the occurrence of singularity that appears when evaluation point lies directly on the vortex line.

In order to decrease the computational time, a simplified free wake vortex lattice method similar to [13, 15] is coded and used. Blade is presented by a single row of ring vortices while the wake behind it is modeled by a 3D sheet of ring vortices. The flow is assumed as steady and the mutual effect of blades is neglected.

Induced velocities depend on geometries and intensities of vortex rings presenting the blade and the wake. Total velocity induced by a rectilinear vortex ring can be computed by summing the velocities induced by the four comprising segments. Numerical model of the blade consists of radially, non-uniformly distributed panels positioned on the first quarter of the chord, Figure 4. Bound vortex ring described by circulation Γ_b and a control point CP located at the middle of the panel are assigned to each panel. Curvature of the blade is taken into account through definition of the vectors perpendicular to camber line of each airfoil at 3/4 of chord length (at control points).

Boundary conditions established so that the normal velocity component equals zero at each control point result in a system of linear equations that can be solved to find the unknown distribution of circulation over the blade:

$$\begin{bmatrix} a_{11} & a_{12} & \cdots & a_{1n} \\ a_{21} & a_{22} & \cdots & a_{2n} \\ \vdots & \vdots & \ddots & \vdots \\ a_{n1} & a_{n2} & \cdots & a_{nn} \end{bmatrix} \begin{bmatrix} \Gamma_1 \\ \Gamma_2 \\ \vdots \\ \Gamma_n \end{bmatrix} = \begin{bmatrix} -(\mathbf{V}_0 + \boldsymbol{\Omega} \times \mathbf{r} + \mathbf{v}_i)_1 \cdot \mathbf{n}_1 \\ -(\mathbf{V}_0 + \boldsymbol{\Omega} \times \mathbf{r} + \mathbf{v}_i)_2 \cdot \mathbf{n}_1 \\ \vdots \\ -(\mathbf{V}_0 + \boldsymbol{\Omega} \times \mathbf{r} + \mathbf{v}_i)_n \cdot \mathbf{n}_1 \end{bmatrix}$$

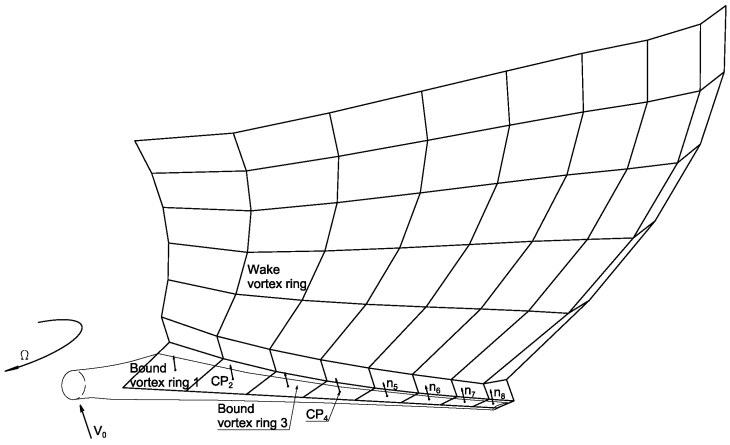

FIGURE 4. Blade model, bound and wake vortex rings, control points CP_i and panel normals $\mathbf{n}_i$

Equations are defined in a body-fixed coordinate system so that influential coefficients a_{ij} can be defined only once at the beginning of the computation (when there are still neither wake nor induced velocities from the wake). Kutta (trailing edge) condition is satisfied by imposing the requirement that the strengths of trailing vortex rings equal the strengths of bound vortex rings in the previous time-step:

$$\Gamma_{w,i}(t + \mathrm{d}t) = \Gamma_{b,i}(t).$$

After the computation of the new values of bound circulation, wake displacement is realized as:

$$\mathbf{V}_{\mathrm{tot}} = \mathbf{V}_0 + \mathbf{v}_{i,b} + \mathbf{v}_{i,w},$$
$$\mathbf{r}(t + \mathrm{d}t) = \mathbf{r}(t) + \mathbf{V}_{\mathrm{tot}}\Delta t.$$

The whole, constantly increasing sheet of wake vortices is moved in every iteration. Once the velocity field around the blade is determined, again through the use of Kutta–Joukowski theorem, it is possible to estimate the lift force acting on the blade segment. The values of local inflow angles α are calculated from the computed distribution of circulation. Using the available 2D airfoil characteristics leads to an estimation of the drag force acting on the blade segment. Once the lift and drag forces are known, the normal and tangential force components can easily be computed.

3.3. RANS set-up. Flow field can also be modeled by Reynolds Averaged Navier–Stokes (RANS) equations closed by one of the usually employed turbulence models based on the assumption of isotropic turbulence. Here, numerical simulations were performed in ANSYS FLUENT 16.2 where governing flow equations for incompressible, viscous fluid are solved by finite-volume method.

3.3.1. *Geometry description.* Rotor model consists of 3 isolated blades. Blade model is simplified. It corresponds to the original blade geometry in the span of 20–100% meaning that the root segment is cut-off, Figure 2b.

Computational domain comprises two zones: rotor and stator. Rotor is shaped like a cylinder encompassing the blades (in yellow color in Figure 5). Similar to [8], its diameter is 37.5% greater than turbine diameter. It extends for $0.25R$ (rotor radius) before and $2.25R$ behind the blades. The stationary outer domain, stator, is also a cylinder stretching -5 and $+10$ blade lengths along z-axis (wind speed direction) respectively and approximately 3.5 blade lengths in two other directions forming the transverse plane (the rotor plane).

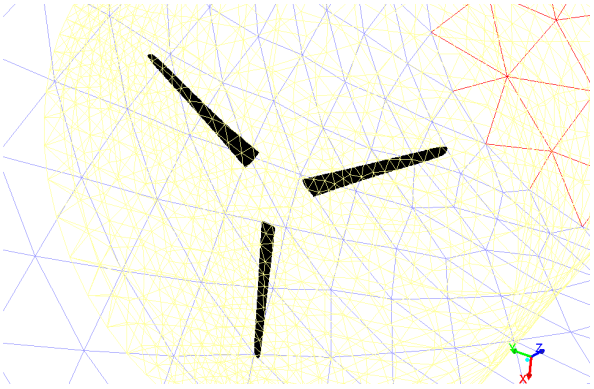

FIGURE 5. Computational mesh: velocity inlet (blue), pressure outlet (red), blades (black), rotor–stator interface (yellow)

3.3.2. *Grid generation.* Computational mesh used in simulations was adopted after a grid convergence study. It is hybrid unstructured and contains approximately 2.7 million cells, Figure 5. Twenty layers of refined prismatic cells encompass the surfaces of the blades. Dimensionless wall distance is below 1.5, $y^+ < 1.5$. Both pressure and suction surfaces of the blades are mapped with rectangles. Numbers of divisions in the span-wise and chord-wise directions are 100 and 50 respectively. Cells grow larger towards the domain outer boundaries.

3.3.3. *Numerical setting and boundary conditions.* Steady or unsteady RANS equations were closed by either a two-equation $k-\omega$ SST, a combination of standard $k-\omega$ model near the walls and $k-\epsilon$ in the outer layer, or a four-equation $\gamma - \mathrm{Re}_\theta$ turbulence model specially developed for transitional flows. The latter model is derived from the former with 2 additional equations for intermittency γ and momentum thickness Reynolds number $\mathrm{Re}_{\theta t}$. Fluid, air, was considered as incompressible gas of constant dynamic viscosity.

Dirichlet boundary conditions concerning velocity and turbulence quantities are imposed on inlet and outlet boundaries. No-slip boundary conditions are defined on blade surfaces. Angular velocity $\Omega = 324.5$ RPM is assigned to rotor zone.

Flow around an isolated wind turbine rotor can be simulated as a steady flow in a rotating frame of reference with the mean time-averaged parameters as outputs.

However, if real-time load distributions are of interest it is necessary to employ a moving mesh approach where periodic unsteadiness during one rotation can be more accurately captured. Both possibilities are tested and compared in the study.

Pressure-based SIMPLE scheme is used for solving the flow equations. Gradients are obtained by the least squares cell-based method. Spatial discretizations are of the second order. Where needed (unsteady simulations of isolated rotor in the sliding mesh approach), temporal discretization is of the first order with the time-step corresponding to a 1/360 of the rotation period.

4. Numerical results and discussion

Computed numerical results are compared to available MEXICO wind tunnel data. Obtained power and thrust force curves as functions of tip-speed ratio are illustrated in Figures 6 and 7.

Looking at the power coefficient, when the two first, simpler approaches are analyzed, it can be concluded that the trend of the relation is captured, although the numerical values are overestimated. However, it should be emphasized that

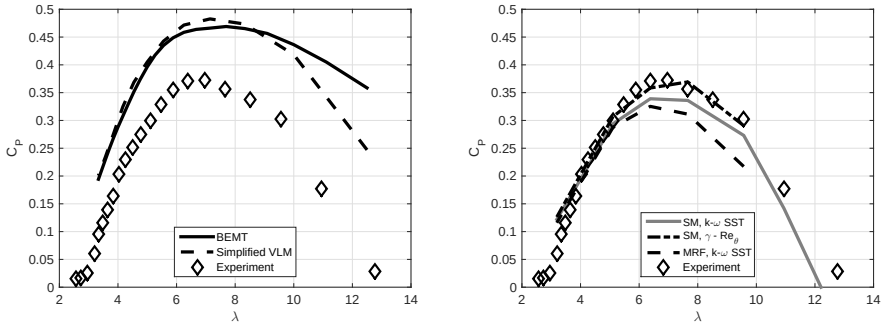

FIGURE 6. Power coefficient curve over a range of tip-speed ratios

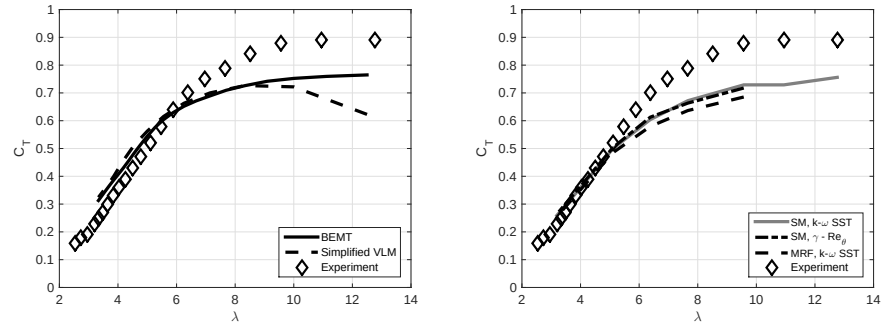

FIGURE 7. Thrust force coefficient curve over a range of tip-speed ratios

the investigated numerical approaches use simplified, adapted 2D experimentally obtained airfoil characteristics. Furthermore, these models mostly neglect viscous drag and Reynolds number effects.

On the other hand, with RANS approach, the tested numerical settings produce tolerably underestimated rotor performance. However, numerical results obtained by $\gamma - \mathrm{Re}_\theta$ model can be considered quite satisfactory when power coefficient is concerned. Both curve trend and maximal values are well captured. $k - \omega$ SST provides somewhat smaller values than experimentally measured. This can be explained by the fact that the four-equation model better simulates dynamic stall and flow reattachment. As expected, sliding mesh approach performs better in comparison to the rotating frame of reference.

At higher values of tip-speed ratio (smaller wind speeds), all tested models failed to adequately capture the thrust force coefficient and returned lower values. However, at the range of nominal wind speeds $V_0 \in [10, 25]$m/s values corresponding well to experimental are obtained. Another way to test the two simpler models is to compare distributions of normal force F_N along the blade, Figure 8. As expected, greatest values occur near the blade tip.

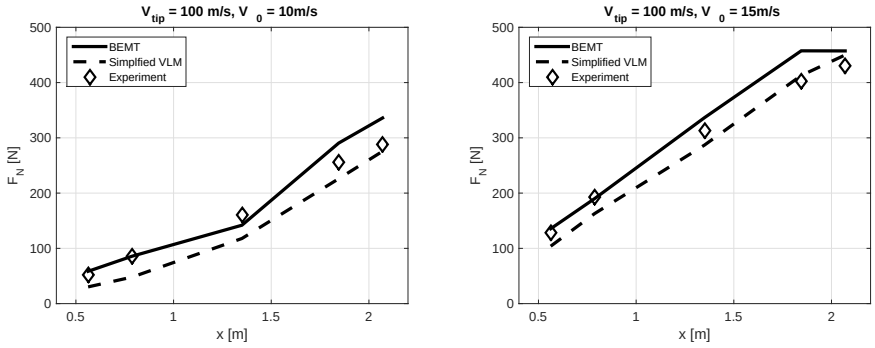

FIGURE 8. Normal force distribution along the blade at $V_0 = 10\,\mathrm{m/s}$ (left) and $V_0 = 15\,\mathrm{m/s}$ (right)

Wake shapes at $V_0 = 15\,\mathrm{m/s}$ computed by the simplified VLM and RANS $\gamma - \mathrm{Re}_\theta$ model are illustrated in Figure 9. The correspondence between the wake shapes is good. Wake expansion as well as the grouping of the tip vortices is well captured.

Uneven pressure distribution can be better comprehended by comparing sectional pressure distributions. Figure 10 illustrates the values of pressure at five different spanwise locations $x/R = [0.25, 0.35, 0.60, 0.82, 0.92]$ at three characteristic wind speeds that correspond to quite different operational regimes resulting in remarkably different flow fields, Figure 11. At lower wind speeds, there is no separation whilst at higher wind velocities separation becomes increasingly important and vortex shedding occurs. At these regimes there are notable discrepancies between RANS results and more advanced numerical techniques [3]. Presented results are obtained by $\gamma - \mathrm{Re}_\theta$ turbulence model.

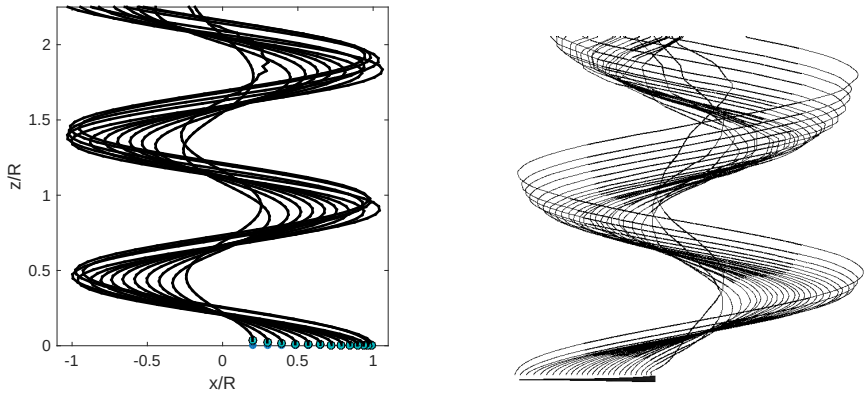

FIGURE 9. Wake behind the blade at $V_0 = 15\,\mathrm{m/s}$ by VLM (left) and RANS (right)

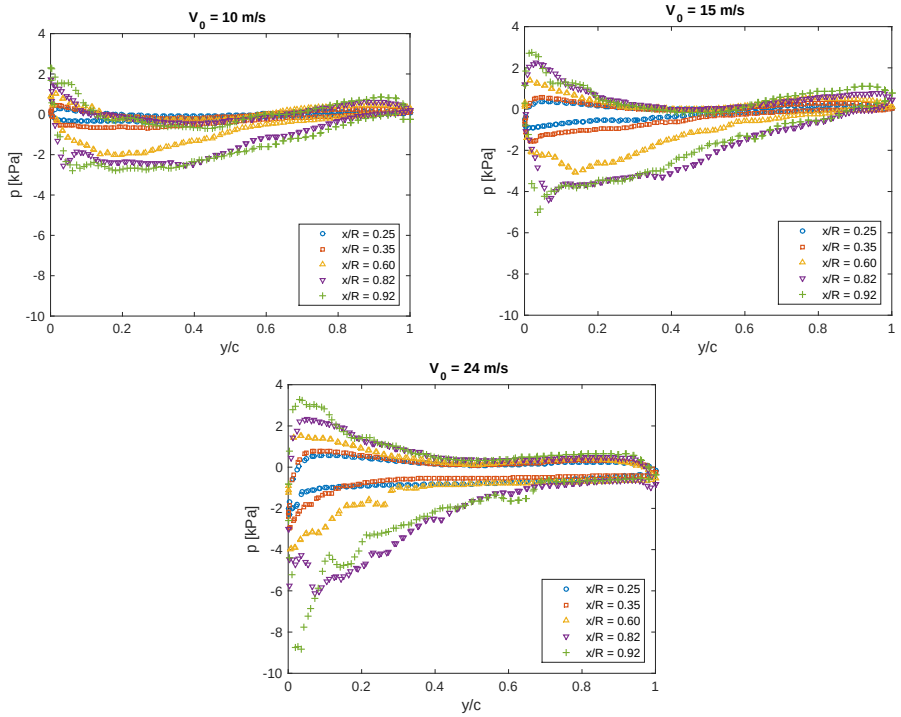

FIGURE 10. Chordwise pressure distribution [Pa] at five different spanwise locations at $V_0 = 10\,\mathrm{m/s}$, $V_0 = 15\,\mathrm{m/s}$ and $V_0 = 24\,\mathrm{m/s}$

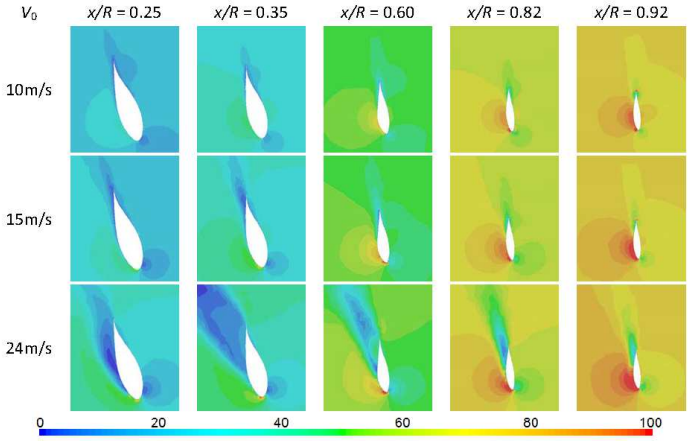

FIGURE 11. Relative velocity contours [m/s] at different wind speeds and spanwise locations

5. Conclusions

Several different numerical models for computation of wind turbine aerodynamic performances have been tested and compared. The most obvious conclusions can be summed up as follows.

BEMT is by far the fastest approach and produces satisfying results. It can, with sufficient reliability, be used for preliminary assessments and when a large number of computations is necessary. However, if velocity field around the turbine is also of interest, one of the vortex methods should be employed. Although fluid viscosity is neglected, quite accurate information on turbine wake can be obtained.

Simplified vortex lattice method seems sufficiently accurate. It seems able to simulate a wider range of operational regimes than BEMT. It is much simpler than CFD techniques, and its performance can be immensely improved by employing parallel computing techniques [14] or by increasing the number of panels in the chordwise direction. The model can be used for obtaining the velocity or vorticity fields since wake structures seem consistently simulated. Tip vortices gather together and evolve as expected.

With RANS equations, Frame of reference approach has the advantage of a much shorter computational time [5]. However, the results it offers are averaged values that can be of somewhat decreased accuracy. It should be used with care for the purpose of initial performance estimation. Furthermore, with this approach the employed turbulence model seems to be of secondary importance (since the two tested models provided quite similar results).

Conclusions are somewhat different for Sliding mesh approach. The numerical data on power (i.e. torque, i.e. tangential force) obtained by the two turbulence models are dissimilar. The most satisfactory correspondence to experimental values was achieved by Sliding mesh approach and $\gamma - \mathrm{Re}_\theta$ turbulence model. Neither of

the models was able to accurately represent the thrust force coefficient which might be attributed to the adopted simplifications in geometry.

Although slight differences in real and model geometry are partially responsible for inconsistencies of two sets of results, none of the employed models can fully capture the complexity of the flow. The difficulty and extreme challenges of modeling (the relevant scales of) turbulence required to accurately model the flow around wind turbines are obvious [2]. Quite refined computational meshes and small time-steps present just an initial requirement. Furthermore, better knowledge and understanding of turbulence is necessary. It can with certainty be concluded that turbulence can greatly affect the wind turbine aerodynamics.

Acknowledgments. The research work is funded by the Ministry of Science, Education and Technological Development of the Republic of Serbia through Technological Development Project no. 35035.

References

1. P. E. Rethore, N. N. Sorensen, F. Zahle, A. Bechmann, H. Madsen, *MEXICO Wind Tunnel and Wind Turbine modelled in CFD*, 29th AIAA Applied Aerodynamics Conference, Honolulu, Hawaii, 2011.
2. J. W. Naughton, J. W. Balas, H. Gopalan, C. Gundling, S. Heinz, R. Kelly, W. Lindberg, R. Rai, J. Sitaramantt, M. Singh, *Turbulence and the isolated wind turbine*, 6th AIAA Theoretical Fluid Mechanics Conference, Honolulu, Hawaii, 2011.
3. Y. Li, K. J. Paik, T. Xing, P. M. Carrica, *Dynamic overset CFD simulations of wind turbine aerodynamics*, Renewable Energy **37** (2012), 285–298.
4. J. G. Schepers, *Engineering models in wind energy aerodynamics*, Ph. D. thesis, Delft University of Technology, Delft, Netherlands, 2012.
5. S. K. Yeom, T. J. Kang, W. G. Park, *Aerodynamic Design of* 2.5 MW *Horizontal Wind Turbine Blade in Combination with CFD Analysis*, ASEM 2013 (Advances in Structural Engineering and Mechanics), Jeju, Korea, 2013.
6. M. Carrion, R. Steijl, M. Woodgate, G. N. Barakos, X. Munduate, S. Gomez-Iradi, *Aeroelastic analysis of wind turbines using a tightly coupled CFD–CSD method*, J. Fluids Struct. **50** (2014), 392–415.
7. W. Y. Zhu, W. Z. Shen, J. N. Sorensen, *Integrated airfoil and blade design method for large wind turbines*, Renewable Energy **70** (2014), 172–183.
8. B. Plaza, R. Bardera, S. Visiedo, *Comparison of BEM and CFD results for MEXICO rotor aerodynamics*, J. Wind Eng. Ind. Aerodyn. **145** (2015), 115–122.
9. Y. Yang, C. Li, W. Zhang, J. Yang, Z. Ye, W. Miao, K. Ye, *A multi-objective optimization for HAWT blades design by considering structural strength*, J. Mech. Sci. Technol. **30** (2016), 3693–3703.
10. *Guidelines for Design of Wind Turbines*, 2nd ed., DNV/Risø, Copenhagen, 2002.
11. A. A. Afjeh, T. G. Jr. Keith, *A Simplified Free Wake Method for Horizontal-Axis Wind Turbine Performance Prediction*, J. Fluids Eng. **108** (1986), 400–406.
12. P. Pratumnopharat, *Novel Methods for Fatigue Data Editing for Horizontal Axis Wind Turbine Blades*, Ph. D. thesis, University of Northumbria, Newcastle, UK, 2012.
13. H. Abedi, *Development of Vortex Filament Method for Wind Power Aerodynamics*, Ph. D. thesis, Chalmers University of Technology, Gothenburg, Sweden, 2016.
14. N. B. deVelder, *Free Wake Potential Flow Vortex Wind Turbine Modeling: Advances in Parallel Processing and Integration of Ground Effects*, M. Sc. thesis, University of Massachusetts Amherst, USA, 2014.
15. J. Katz, A. Plotkin, *Low-speed Aerodynamics: From Wing Theory to Panel Methods*, McGraw-Hill Series in Aeronautical and Aerospace Engineering, New York, 1991.

ПРОЦЕНА АЕРОДИНАМИЧКИХ ПЕРФОРМАНСИ ЛОПАТИЦЕ ВЕТРОТУРБИНЕ ДОБИЈЕНИХ РАЗЛИЧИТИМ ПРОРАЧУНСКИМ МЕТОДАМА

Резиме. Иако су веома заступљени, системи за искоришћење енергије ветра представљају незавршену и савремену тему многих научних студија. На почетку пројектовања, треба посветити нарочиту пажњу аеродинамичкој анализи с обзиром да глобалне перформансе ветротурбине директно зависе од аеродинамичких. И даље је у употреби неколико прорачунских модела различитих по сложености и потребним прорачунским ресурсима. Најчешћи приступи укључују: i) моделе засноване на закону одржања количине кретања, ii) моделе за прорачун потенцијалног струјања и iii) методе прорачунске механике флуида.

У раду су приказана кратка објашњења, преглед и поређење постојећих метода. Једноставнији модели су описани и имплементирани док су бројне нумеричке симулације изолованог ротора са хоризонталном осом обртања који садржи три лопатице извршене у програмском пакету ANSYS FLUENT 16.2. Струјно поље је моделирано Навије-Стоксовим једначинама осредњеним Рејнолдсовом статистиком и затвореним употребом два различита турбулентна модела.

Резултати, укључујући глобалне као што су коефицијент вучне силе или снаге али и локалне расподеле по лопатици, добијени различитим моделима су упоређени са доступним експерименталним подацима. Приказане су визуелизације струјног поља у виду контура брзине, расподеле притиска у различитим попречним равнима и вредности коефицијента снаге и вучне силе за опсег радних режима. Иако је тачност добијених резултата различита, сви разматрани нумерички модели мало потцењују или прецењују глобалне параметре ветротурбине. Турбуленција значајно утиче на аеродинамику ветротурбина и треба је пажљиво моделирати.

Faculty of Mechanical Engineering
University of Belgrade
Belgrade
Serbia
jsvorcan@mas.bg.ac.rs

Faculty of Mechanical Engineering
University of Belgrade
Belgrade
Serbia
opekovic@mas.bg.ac.rs

Faculty of Mechanical Engineering
University of Belgrade
Belgrade
Serbia
tivanov@mas.bg.ac.rs

(Received 30.11.2017.)
(Available online 17.04.2018.)